

Control Design for Variations in Structural Natural Frequencies

Gary J. Balas*

University of Minnesota, Minneapolis, Minnesota 55455

and

Peter M. Young†

Massachusetts Institute of Technology, Cambridge, Massachusetts 02139

The lightly damped nature of flexible structures can lead to controllers that are highly sensitive to modeling errors in structural natural frequencies and damping levels. An approach to directly incorporating these modeling errors into the control design process is presented that leads to less sensitive and more robust controllers with improved performance. This approach is used to synthesize controllers for the NASA Langley Mini-Mast experimental structure. The resulting designs obtain good performance in the presence of significant modeling errors in the structural natural frequencies.

I. Introduction

MATHEMATICAL models of a flexible structure are often derived using finite element methods and refined based on experimental data. A characteristic of these models is that the low-frequency properties of the structure are more accurately described than the higher modes. Increasingly stringent performance requirements on current and future space structures will require active control of a number of low-frequency modes while not destabilizing higher frequency modes. Therefore, not only is improving the initial mathematical model important, but accurately accounting for the inevitable errors in these models plays an increasingly prominent role in the control of lightly damped, flexible space structures.

A number of researchers have addressed controller synthesis for flexible structures in the presence of neglected or unmodeled dynamics.^{1–3} This paper addresses, in addition to unmodeled dynamics, the synthesis of controllers for vibration attenuation that are robust to modeling errors inside the controller bandwidth. These modeling errors can take the form of inaccurate model shape descriptions, errors in the structural natural frequencies and dynamics, as well as neglected actuator and sensor dynamics. An approach to control design for flexible structures based on the μ framework is proposed that directly incorporates knowledge of modeling errors in the natural frequencies in the problem formulation. Experimental and theoretical results are presented that clearly show the power of the μ framework for synthesizing controllers robust to natural frequencies errors.

Aspects of controller synthesis in the presence of natural frequency and damping errors have been addressed by a number of researchers in the control of flexible-structures area. Collins et al.⁴ uses a maximum-entropy approach to synthesize controllers robust to natural frequency. This work employs parameter-dependent Lyapunov functions and Popov's criterion to include real parameter uncertainty into the problem formulation. How and Hall⁵ present an alternative approach to synthesis based on the Popov criterion. They design controllers using a nonlinear search algorithm to optimize robustness and performance simultaneously.

The inclusion of real parameter uncertainty directly into the D - K iteration framework was proposed by Young.⁶ This method introduces an additional G scaling into the design process. Safanov and Chiang⁷ present a method for control design based on optimization techniques that is similar to D - K iteration. Their problem

formulation incorporates parameter uncertainty into the optimization problem governing the control design process. Standard D - K iteration control design is used by Smith et al.⁸ and Balas⁹ with errors in natural frequencies modeled as perturbations in the state-space representation of the plant. These perturbations are written as a linear fractional transformation in the state matrix, and μ -synthesis techniques are used to synthesize controllers for the resulting systems. These methods are similar to those presented here.

This paper adds to the literature by presenting a detailed discussion on how to model and analyze errors in natural frequency using newly developed real/complex structured singular value (μ) algorithms. This allows for the treatment of the real parameter variations in a less conservative manner. Furthermore, a comprehensive study of the importance of including modeling error information in the control problem formulation is presented along with theoretical and experimental validation of the resulting controllers. Using this approach, high-performance controllers are synthesized for an experimental structure in the presence of significant errors in the structural natural frequencies.

The NASA Langley Mini-Mast facility is used as an experimental testbed to verify our approach. Section II provides a brief description of the Mini-Mast facility for the context of this work. The vibration attenuation control objectives, performance specifications, and levels of modeling error are also outlined in this section. A more detailed description of the Mini-Mast facility can be found in the references.^{4,10–12} The structured singular value framework is described in Sec. III. Real/complex μ theory, used to analyze the closed-loop system in the presence of real natural frequency variations and unstructured complex uncertainty, is presented. Controller synthesis via D - K iteration is also briefly described.

Modeling natural frequency errors in the μ framework is discussed in Sec. IV. Natural frequency uncertainty is first posed as parametric uncertainty in a state-space model of the structure and written as linear fractional transformation. The relationship between parametric uncertainty and uncertainty in structural natural frequencies is addressed in Sec. IV.

Formulation of the Mini-Mast control problem in the presence of natural frequency variations is described in Sec. V. The control problem involves perturbing the natural frequencies of the nominal Mini-Mast structure and modeling these errors in the μ framework. Input, natural frequency, unmodeled dynamics uncertainty, and performance weights are presented. Five controllers are synthesized for the system using D - K iteration. Section VI contains the evaluation of these controllers via theoretical analysis, time simulation, and implementation on the Mini-Mast experiment. Results of this work are summarized in Sec. VII.

II. Mini-Mast Facility

The Mini-Mast facility, part of the Control/Structures Interaction Guest Investigator Program, is used to validate the control design

Received Sept. 30, 1993; revision received Oct. 17, 1994; accepted for publication Oct. 19, 1994. Copyright © 1994 by Gary J. Balas and Peter M. Young. Published by the American Institute of Aeronautics and Astronautics, Inc., with permission.

*Assistant Professor, Department of Aerospace Engineering and Mechanics. Member AIAA.

†Post Doctoral Associate, Laboratory for Information and Decision Systems.

approach proposed in this paper. It consists of a deployable and retractable beam truss designed to represent future deployable space trusses.^{4,10,11} The Mini-Mast is an 18-bay, 20.16-m-long truss beam structure cantilevered at its base from a rigid foundation. The structural members of the truss are made of a graphite/epoxy composite material with joints composed of titanium and stainless steel. A cable is attached to the tip of the Mini-Mast structure to off-load the 350-lb tip mass.

The Mini-Mast facility is instrumented with 51 displacement sensors, three rate gyros at bay 18, and six accelerometers. Four of the accelerometers are located on bay 18 and two on bay 10. In addition, there are six actuators on the structure. The three control actuators are located on bay 18 and the three disturbance actuators are located at bay 9.

The three torque wheel actuators (TWAs) used for control are located at the tip platform (bay 18) and are mounted in the x , y , and z directions. They are denoted TWAX, TWAY, and TWAZ, respectively. The TWA transfer functions between voltage and torque are represented by second-order transfer functions, $Ks/(s + \alpha)(s + \beta)$, where $K \approx 36,000$, $\alpha = 23.5$, and $\beta = 370$.

The TWAs can saturate since the input voltage is restricted to between ± 50 V. This effectively limits the current to the motor, with the back electromotive force (emf) limiting the speed to 62 rpm. The disturbance excitations enter the structure via three 50-lb shakers attached at bay 9 of the structure. The shakers are represented as constants since their bandwidth is far above the bandwidth of the system.

Accelerometer and displacement sensors located on bays 10 and 18 are available for feedback. The accelerometers (Sunstrand QA-1400) have a bandwidth of 0–200 Hz and very low noise characteristics. There are a total of six accelerometers, four of them are located on the tip platform (bay 18) and two of them are located at the midplatform (bay 10). There are three Kaman displacement sensors located at bays 10 and 18. These are mounted on a support structure parallel to the Mini-Mast platform faces and measure displacement normal to the probe. The Kaman sensors have a range of ± 1 in. at bay 10 and ± 2 in. at bay 18. They are scaled to ± 1 and ± 0.5 mV/mil at bays 10 and 18, respectively.

In this paper, only bay 18 accelerometers are used for feedback control. Results of a previous study in Ref. 12 indicated that using only bay 18 accelerometers on the Mini-Mast structure for feedback, with performance specifications on bays 10 and 18, all the desired characteristics and observations are incorporated in the control design problem. Bay 10 and 18 displacement sensors are used only as a performance measure. All the sensors are filtered through a third-order, 10-Hz Bessel filter prior to digitization.

A. Structural Model

A Nastran finite element model of the Mini-Mast structure was developed and refined by NASA Langley engineers.¹¹ From this model, a 28-mode, 6-input, 10-output simulation model was synthesized. Both models correlate well with low-frequency experimental data. The inputs to the structure are the three control actuators and three disturbance actuators. The output measurements are the three displacement measurements at bays 18 and 10 and the four accelerometers at bay 18. Small deviations are noted between the 28-mode simulation model and physical system. These are attributed to a higher level of damping present in the actual structure compared with the model. Little error is observed in the first five-mode natural frequencies to be controlled.

A reduced-order model of the Mini-Mast structure is formulated for control design based on the first five modes of the structure. These modes, shown in Table 1, are to be actively controlled.^{4,10,12} The remaining 23 modes, between 92.5 and 460.8 rad/s, are accounted for in the control design as unmodeled dynamics. Transfer function magnitude plots of the 5- and 28-mode models from the TWAs to the bay 18 accelerometers are shown in Fig. 1.

B. Control Objectives

The control objective for the Mini-Mast structure is to attenuate structural vibration at bays 10 and 18 due to input disturbances at

Table 1 Natural frequencies, damping levels, and modes of Mini-Mast structure

Mode number	Theoretical frequency, rad/s	Theoretical damping level, %	Mode description
1	5.12	1.8	First Y bending
2	5.12	1.8	First X bending
3	27.46	1.2	First torsional
4	40.09	1.0	Second Y bending
5	40.46	1.0	Second X bending

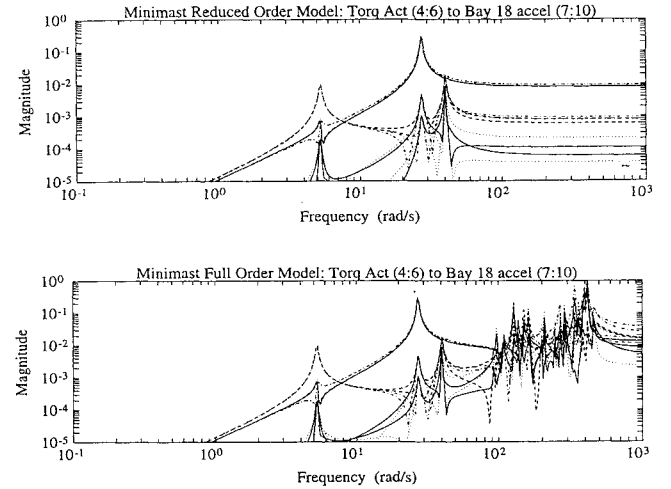


Fig. 1 Transfer function magnitudes from torque actuators to bay 18 accelerometers.

bay 9. The controllers use bay 18 acceleration measurements for feedback. The TWAs used for control are also located at bay 18, though they are not collocated with the sensors. Hence, this control problem includes both noncollocated feedback sensors, though on the same bay platform, and noncollocated performance specifications on bay 10 and 18 displacements. The controllers need to be insensitive to variations between the physical structure and its mathematical model.

The accuracy of the Mini-Mast model lends itself to addressing the issue of designing controllers for flexible structure in the presence of natural frequency variations. The Mini-Mast model is treated as the actual or real structure in the design process since it is highly accurate in the frequency range where performance is desired. Another mathematical model is constructed, which varies from the accurate finite element model in a predefined manner, and used as the control design model. As an example, one control design model has each of the first five natural frequencies of the design model perturbed by $\pm 2.5\%$. A controller is synthesized based on the perturbed design model and implemented on the original finite element model. The same controller is also implemented on the physical system. The variations or errors in the natural frequencies are accounted for in the control design process with structured parametric uncertainty models.

III. Structured Singular Value

In order to accurately analyze the robustness properties of our system with uncertain natural frequencies, we will need to consider a structured singular value (μ) analysis problem with real and complex uncertainty. This *mixed* μ problem (the uncertainties are allowed to be real or complex) can be quite different to its more familiar *complex* μ counterpart (all uncertainties are treated as complex), and we will briefly review some of the main analysis results (see also Refs. 13 and 14).

First we define the mixed μ problem. Given three nonnegative integers m_r , m_c , and m_C , let $m := m_r + m_c + m_C$, and define the block structure $\mathcal{K}(m_r, m_c, m_C)$ as an m -tuple of positive integers

$$\mathcal{K} = (k_1, \dots, k_{m_r}, k_{m_r+1}, \dots, k_{m_r+m_c}, k_{m_r+m_c+1}, \dots, k_m) \quad (1)$$

where $n \doteq \sum_{i=1}^m k_i$. This determines the set of allowable perturbations, namely define

$$\begin{aligned} X_K &= \left\{ \Delta = \text{block diag}(\delta_1^r I_{k_1}, \dots, \delta_{m_r}^r I_{k_{m_r}}, \delta_1^c I_{k_{m_r+1}}, \dots, \right. \\ &\quad \left. \delta_{m_c}^c I_{k_{m_r+m_c}}, \Delta_1^C, \dots, \Delta_{m_c}^C) : \delta_i^r \in \mathbb{R}, \delta_i^c \in \mathbb{C}, \right. \\ &\quad \left. \Delta_i^C \in \mathbb{C}^{k_{m_r+m_c+i} \times k_{m_r+m_c+i}} \right\} \end{aligned} \quad (2)$$

Note that the full complex blocks need not in fact be square, but we restrict them as such to simplify the presentation. All of the results that follow can easily be modified to handle nonsquare blocks, and in fact, the software for computing the bounds handles the more general case.^{6,15}

Definition 1. The structured singular value $\mu_K(M)$ of a matrix $M \in \mathbb{C}^{n \times n}$ with respect to a block structure $K(m_r, m_c, m_C)$ is defined as

$$\mu_K(M) = \left(\min_{\Delta \in X_K} \{ \bar{\sigma}(\Delta) : \det(I - \Delta M) = 0 \} \right)^{-1} \quad (3)$$

with $\mu_K(M) = 0$ if no $\Delta \in X_K$ solves $\det(I - \Delta M) = 0$.

Note that this definition of μ is identical with the usual one,^{16,17} except that the allowable perturbation set X_K has been modified to allow (repeated) real scalar blocks. New upper and lower bounds for mixed μ problems are required. Define the following sets of block-diagonal scaling matrices:

$$\begin{aligned} Q_K &= \left\{ \Delta \in X_K : \delta_i^r \in [-1 \ 1], \delta_i^c \delta_i^c = 1, \right. \\ &\quad \left. \Delta_i^{C*} \Delta_i^C = I_{k_{m_r+m_c+i}} \right\} \end{aligned} \quad (4)$$

$$\begin{aligned} \mathcal{D}_K &= \left\{ \text{block diag}(D_1, \dots, D_{m_r+m_c}, d_1 I_{k_{m_r+m_c+1}}, \dots, d_{m_c} I_{k_m}) : \right. \\ &\quad \left. 0 < D_i = D_i^* \in \mathbb{C}^{k_i \times k_i}, 0 < d_i \in \mathbb{R} \right\} \end{aligned} \quad (5)$$

$$\begin{aligned} \mathcal{G}_K &= \left\{ \text{block diag}(G_1, \dots, G_{m_r}, O_{k_{m_r+1}}, \dots, O_{k_m}) : \right. \\ &\quad \left. G_i = G_i^* \in \mathbb{C}^{k_i \times k_i} \right\} \end{aligned} \quad (6)$$

Then we have the following upper and lower bounds for mixed μ :

Theorem 1 (lower bound¹⁴). For any matrix $M \in \mathbb{C}^{n \times n}$ and any compatible block structure K ,

$$\max_{Q \in Q_K} \rho_R(QM) = \mu_K(M) \quad (7)$$

Theorem 2 (upper bound¹³). For any matrix $M \in \mathbb{C}^{n \times n}$ and any compatible block structure K ,

$$\begin{aligned} \mu_K(M) &\leq \inf_{\substack{D \in \mathcal{D}_K \\ G \in \mathcal{G}_K}} \left[\min_{\substack{\beta \in \mathbb{R} \\ \beta \geq 0}} \left\{ \beta : [M^* D M + j(GM - M^* G) \right. \right. \\ &\quad \left. \left. - \beta^2 D] \leq 0 \right\} \right] \end{aligned} \quad (8)$$

Theorems 1 and 2 give us the basis of computation schemes for upper and lower bounds for mixed μ problems. These have been implemented as a MATLAB function in Version 2.0 of the μ Analysis and Synthesis Toolbox (μ -Tools), which is used to compute all the mixed μ analysis results in this paper.¹⁵ The frequency-domain use of μ to examine robust stability and robust performance problems is still valid for mixed μ problems.¹⁸ Mixed μ plots can still be used as a necessary and sufficient test for robust performance with linear, time-invariant perturbations, but now including real parameter variations in the uncertainty description. This enables us to handle the robustness analysis of our system with respect to natural frequency variations in a less conservative manner.

The control design approach used is complex μ synthesis (for recent developments in mixed μ synthesis see Refs. 5–7). This approach attempts to minimize the complex μ upper bound since minimizing μ directly is too difficult. Note that by so doing we are covering the real parameters with complex uncertainty for design

purposes. Since this clearly has the potential to introduce conservatism into our controller design, the resulting closed-loop systems will be analyzed with the mixed μ functions described earlier.

A complex μ -synthesis methodology, D - K iteration is used to design controllers to achieve the desired robust performance objectives by integrating H_∞ control design with complex μ analysis.^{5,7,19} The D - K iteration alternately minimizes the complex μ upper bound with respect to K or D holding the other variable constant. Although this iteration scheme is not guaranteed to reach the global optimum, it has been applied successfully to a variety of different aerospace applications.^{3,20,21} More detailed discussions of D - K iteration can be found in the references.^{15,20–23} All controllers are synthesized and analyzed using the μ -Tools software.¹⁵

IV. Parameter Variations

Modeling errors or uncertainties can be described by frequency-domain or parametric uncertainty.^{8,9,16} This paper treats parameter variation in the coefficients of a state-space model as parametric uncertainty. These coefficients are extracted from the system description and rearranged so that the perturbations enter the system in a linear fractional form.²⁴ Sources of parametric uncertainty in flexible structures include the mass, damping, and stiffness coefficients or in modal coordinates the natural frequencies and damping ratios of the structure. These parametric uncertainty models are typically real variations, with the parameters lying within a range of real numbers.

The approach taken in this paper for real parameter variations is to bound them by a complex variation for design purposes. Note that this may introduce additional conservatism into the control design. Therefore, it is important to carefully select the way we cover the real parameters with complex perturbations to reduce the conservatism of their approximation to the real variation. Furthermore, it is important to then analyze the real parameter variations directly to verify that this approximation is valid.

In flexible structures, treating the damping and natural frequency uncertainty individually leads to repeated parametric uncertainties that are undesirable for the current discussion. Hence we will restrict uncertainty to the damping coefficient ζ_i and the natural-frequency-squared term ω_i^2 . Consider a single-mode transfer function, from input force to displacement output, with uncertainty in the damping and natural frequency squared terms:

$$\frac{1}{s^2 + 2\zeta\omega(1 + \delta_1) + \omega^2(1 + \delta_2)} \quad (9)$$

The transfer function can be represented using state-space notation as

$$\left[\begin{array}{c|c} \hat{A} & \hat{B} \\ \hline \hat{C} & \hat{D} \end{array} \right] = \left[\begin{array}{cc|c} 0 & 1 & 0 \\ -\omega^2(1 + \delta_2) & -2\zeta\omega(1 + \delta_1) & 1 \\ \hline 1 & 0 & 0 \end{array} \right] \quad (10)$$

and rewritten in the form

$$\left[\begin{array}{c|c} \hat{A} & \hat{B} \\ \hline \hat{C} & \hat{D} \end{array} \right] = \left[\begin{array}{c|c} A & B \\ \hline C & D \end{array} \right] + \sum_{i=1}^n \delta_i \left[\begin{array}{c|c} A_i & B_i \\ \hline C_i & D_i \end{array} \right] \quad (11)$$

where

$$\left[\begin{array}{c|c} A & B \\ \hline C & D \end{array} \right]$$

represents the nominal state-space system and

$$\left[\begin{array}{c|c} A_i & B_i \\ \hline C_i & D_i \end{array} \right]$$

the perturbed parameters. For a single real parameter, the perturbation matrix is rank 1. Hence in the example stated, the \hat{A} matrix is

$$\hat{A} = \begin{bmatrix} 0 & 1 \\ -\omega^2 & -2\zeta\omega \end{bmatrix} + \delta_1 \begin{bmatrix} 0 \\ 1 \end{bmatrix} [0 \ -2\zeta\omega] + \delta_2 \begin{bmatrix} 0 \\ 1 \end{bmatrix} [-\omega^2 \ 0] \quad (12)$$

The same approach can be expanded upon for any number of perturbations. This technique is used to include parametric uncertainty associated with the state matrix A into the control problem formulation.

Modeling errors in the structural natural frequencies ω_i are described by variations in the natural-frequency-squared coefficients. The modal transfer function from input force to acceleration is described as

$$\frac{b_i c_i s^2}{s^2 + 2\zeta_i \omega_i s + \omega_i^2 (1 + \delta_i)} \quad \text{for} \quad i = 1, 2, 3, 4, 5$$

The perturbations δ_i for each mode are treated as complex uncertainty in the D - K iteration procedure. Therefore, although no uncertainty is included directly in the $2\zeta_i \omega_i s$ term, treating δ_i as complex serves to introduce uncertainty in this term. This is one of the beneficial properties of treating errors in the natural frequencies as frequency-squared complex uncertainty as opposed to a real uncertainty. Uncertainty in the viscous damping level for each mode is advantageous since damping values are difficult phenomena to accurately predict or measure.

One must account for the fact that a variation of α percent in a natural frequency leads to variations of approximately 2α percent in ω_i^2 when the percentage variations are less than 20%. In the subsequent control designs, each of the five natural frequencies of the Mini-Mast control design model are described via uncertainty in ω_i^2 . Two parameters are varied in the control designs: the size of the natural frequency uncertainty and the nominal natural frequencies in the design model.

Four levels of natural frequency uncertainty, $+2.5\%$, $\pm 5.5\%$, and $+10\%$, are used to describe the variation in natural frequency of the nominal model in the control designs. For each level of uncertainty a design model is formulated. Increases in the structural natural frequencies are the most difficult variations to design for, therefore -2.5% and -10% natural frequency variations are not presented. The design model, which is the nominal model in the μ synthesis methodology, takes on the "wrong" nominal natural frequencies at α percent higher or lower than the "true" model natural frequency. The Mini-Mast model provided by NASA Langley researchers is taken to be the true model. By selecting the nominal model natural frequencies to be perturbed by the same amount of parametric

uncertainty, the true model is placed at the extreme of the set of uncertain plant models describing the structural system.

V. Problem Formulation

A set of controllers are designed for plant models with deliberately "incorrect" natural frequencies to mimic the effect of inaccurate models of flexible structures. The design model natural frequencies are assumed to be in error, and this error is covered/covered for by parametric uncertainty models. The controllers are synthesized to be robust to the prescribed natural frequency errors. The controllers are tested and validated on the original "correct" model and on the experimental structure.

Four controllers are designed for four different levels of parametric uncertainty in the natural frequencies, the same for each mode, $+2.5\%$, $\pm 5.5\%$, and $+10\%$. These controllers are denoted Kp2.5, Kp5.5, Kn5.5, and Kp10. Recall that each of the control design models had an incorrect nominal natural frequency at α percent higher or lower than the true model.

A block diagram of the problem formulation is shown in Fig. 2. The control design model, Minim_mr, consists of the first five modes of the Mini-Mast structure. Frequency-squared complex uncertainty is used to account for errors in the structural natural frequencies in all of the control designs discussed in this paper. The natural frequency variations are described by complex perturbations in the μ -synthesis procedure and as real parametric uncertainty in the analysis problem. Here, $\delta_1, \delta_2, \delta_3, \delta_4$, and δ_5 represent variations in the first five natural frequencies, respectively.

There are two sources of complex uncertainty. Uncertainty in the TWA models is represented as a constant, 2% input multiplicative uncertainty to the actuator. This level was determined to be the most suitable input uncertainty description from a performance-vs-robustness study performed on the Mini-Mast facility.¹² $W_{act,out}$ is taken to be 0.02 and $W_{act,in}$ is taken as 1. An additive uncertainty model is included to account for the high-frequency dynamics of the Mini-Mast structural model neglected in the design model and neglected actuator and sensor dynamics. The unmodeled dynamics correspond to the 23 modes between 92 and 461 rad/s. The additive uncertainty weight requires a prescribed level of roll-off of the loop gain, which in effect requires the unmodeled high-frequency structural modes to be gain stabilized by the controllers. This weight is

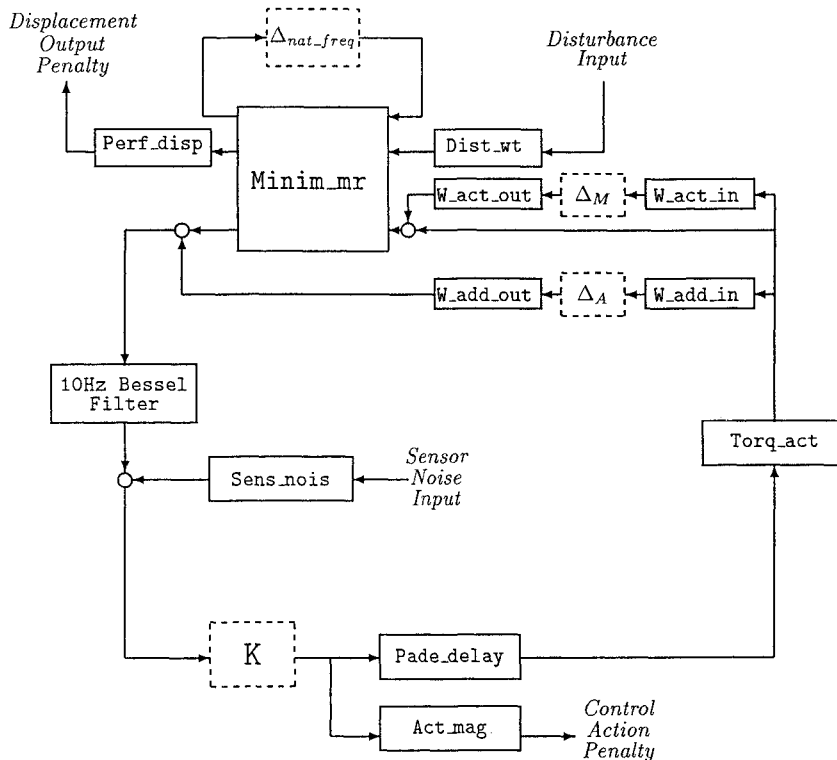


Fig. 2 Control interconnection structure with natural frequency variations.

split into $W_{\text{add.out}}$ and $W_{\text{add.in}}$ to improve the initial H_∞ control problem:

$$W_{\text{add.out}} = \frac{0.25(s^2 + 25.46s + 324)}{s^2 + 1414s + 100,000}$$

$$W_{\text{add.in}} = \frac{77.8(s^2 + 42.43s + 900)}{s^2 + 282.84s + 40,000}$$

Balancing the additive uncertainty weights is not necessary, but it is done to numerically aid the D - K iteration and reduce the order of the D scalings.

The performance specification of attenuating the vibration of the first five modes is introduced into the problem formulation by weights on bay 10 and 18 displacements. The performance weighting functions are scaled such that when the weighted H_∞ norm between the disturbances and displacements is below 1, the desired performance is achieved. The disturbance enters the structure via exciters at bay 9. A frequency-domain weight, Dist.wt equal to $31/(s + 31)$, is used to model the 10-N, 0.1-s impulse disturbance to each exciter. Perf.disp weights on bay 10 and 18 displacements are taken to be 4000 and $20,000(s + 0.5)/(s + 50)$, respectively. The performance objective corresponds to reducing the peaks in the transfer functions between the exciter inputs and displacement outputs. The weighting on the actuator command, Act.mag , is 1. This is similar to allowing the torque actuators to supply a maximum torque of $\pm 8 \text{ N} \cdot \text{m}$ to attenuate the 10-N, 0.1-s impulse disturbance.

The feedback accelerometers are filtered with a third-order, 10-Hz Bessel filter. The Bessel filter is modeled as $(1 - 0.015s)/(1 + 0.015s)$ to account for the low-frequency phase lag of the filter. The phase characteristics play a much more important role in the controller design than their magnitude attenuation. The noise weight on the filtered accelerometers is modeled as 10^{-5} . A Padé delay model, $(1 - 0.005s)/(1 + 0.005s)$, is used to represent the time delay associated with the digital implementation of the control laws at 80-Hz sample rate. A block diagram description of the control problem formulation is shown in Fig. 2.

VI. μ -Synthesis Controller Designs

Four controllers are synthesized for the four different variations in natural frequency of $+2.5\%$, $+5.5\%$, -5.5% , and $+10\%$. All controllers achieved a μ value less than 1 with all of the perturbations blocks treated as complex uncertainties. The nominal interconnection with uncertainty and performance weights has 43 states. Constant D scalings are used for the natural frequency, $\delta_1, \dots, \delta_5$, and multiplicative uncertainty, Δ_M . First-order D scales are used to fit the additive uncertainty data Δ_A . The resulting controller has 49 states.

The state order for controllers Kn5.5, Kp5.5, Kp2.5, and Kp10 after reduction using balanced realization techniques was 11, 18, 34, and 30, respectively. Structured singular value (μ) plots for these controllers are shown in Fig. 3. The structure of the uncertainty description plays a major role in the controller analysis and synthesis. Ignoring the structure of the problem formulation and calculating the maximum singular value from the inputs to the outputs of the closed-loop system with controller Kp10 implemented leads to an H_∞ -norm of 470.

The four controllers are analyzed using the real/complex μ analysis techniques discussed in Sec. III. Recall that complex μ is an upper bound on real/complex μ ; hence the controllers will all have mixed μ values less than 1. For all the mixed and complex μ problems the upper and lower bounds were almost identical across the entire frequency range, so that for clarity of presentation only the upper bound is plotted in each case. Figure 4 is a comparison between complex and real/complex μ of the closed-loop system with controller Kp10 implemented. In the mixed analysis, the parametric uncertainties associated with the frequency-squared variations, $\delta_1, \dots, \delta_5$, are treated as real (as opposed to complex) scalar uncertainties. The two μ plots differ only slightly, indicating that the control design process is not overly conservative in treating the frequency-squared uncertainty as complex rather than real uncertainty. This is the main reason why controllers designed for $\pm 10\%$

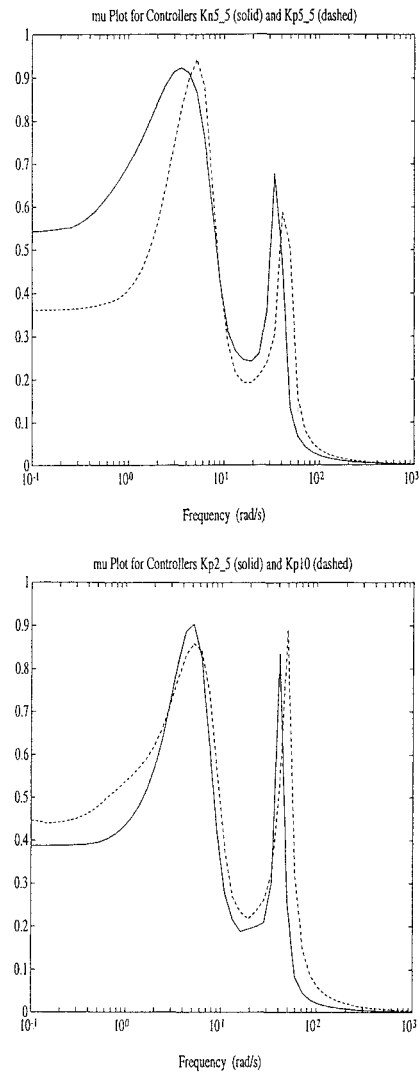


Fig. 3 Complex μ plot of controllers Kn5.5, Kp5.5, Kp2.5, and Kp10.

variation in natural frequencies perform well when implemented on the experimental Mini-Mast structure.

Controller Knom is analyzed for the same problem formulation as is used in the design of controller Kp10 with $+10\%$ variation in the first five natural frequencies. Controller Knom was designed for the block diagram formulation shown in Fig. 2 using the correct Mini-Mast model with no uncertainties in the structural natural frequencies. Therefore, one would expect this controller not to exhibit the same robustness characteristics as controller Kp10. This is in fact the case. The complex and real/complex μ plot of the closed-loop system with Knom implemented, shown in Fig. 4, indicates that there is a perturbation at 40 rad/s (the second bending modes) that would cause significant degradation in performance and robustness of the closed-loop system.

Controller Knom performs well on the Mini-Mast experiment because it was designed using the correct structural model. However, its lack of robustness to natural frequency variations indicates that, if such an accurate model had not been available, the performance would have been poor. In particular, if we had carried out this design using one of the wrong nominal models but without including uncertainty in the natural frequencies, then we would not have obtained a satisfactory design.

The sensitivity of Knom to perturbations in the second bending modes may be explained by the Bode plots of controllers Knom and Kp10 (Fig. 5). Knom has a definite notch in its Bode magnitude plot at approximately 40 rad/s, whereas Kp10 has no notch, as seen in Fig. 5. The μ -synthesis methodology put an approximate notch filter at the second bending modes, since Knom was designed with no parametric uncertainty in the structural natural frequencies. Controller Kp10, which

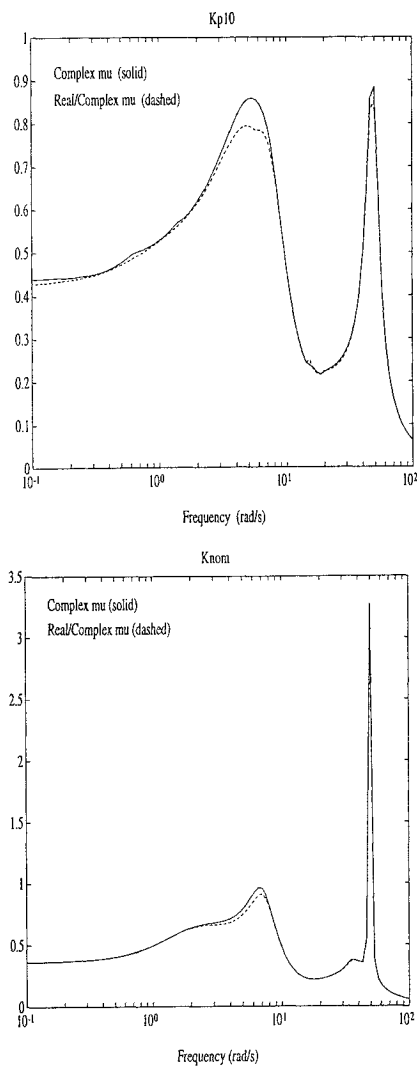


Fig. 4 Complex vs real/complex μ plots for controller Kp10 and Knom with 10% natural frequency uncertainty.

was synthesized by accounting for natural frequency uncertainty, does not try to notch out the second bending mode. Instead, the controller sacrifices performance, in terms of vibration attenuation, by reducing the magnitude of the controller in the 40-rad/s frequency range. This makes Kp10 less sensitive to variations in the natural frequency of this mode with minimal degradation in performance. Hence by accounting for natural frequency variations in the design process, we were able to achieve the desired level of *both* robustness and performance of the Mini-Mast structure in the presence of significant natural frequency variations.

The real/complex μ computational bounds discussed earlier are extremely important in providing the control engineer with a method of determining the effect of real parameter perturbations on the closed-loop system and of finding problem real parameter perturbations for the system. These real parameter perturbations may help the structural designers determine how to better design the structure prior to trying to control it.

Each controller is simulated with the corresponding design model and the true Mini-Mast model. Recall that the control design models have the first five natural frequencies perturbed from the true Mini-Mast model. All the controllers are stable and achieve varying levels of performance on the simulation models. Table 2 contains a list of the open- and closed-loop damping values of the first five modes of the Mini-Mast structure with controllers Kn5.5, Kp5.5, Kp2.5, and Kp10 implemented. Time simulation results, run at 80 Hz sample rate, validate that controllers can be designed to directly incorporate natural frequency uncertainty in lightly damped, flexible-structure control problems.

Controllers Kn5.5, Kp5.5, Kp2.5, and Kp10 are discretized at 80 Hz and implemented on the Mini-Mast experimental structure.

Table 2 Open- and closed-loop damping values with Kn5.5, Kp5.5, Kp2.5, Kp10 implemented on 28-mode simulation model

Controller	Theoretical modal damping percentages				
	Mode 1	Mode 2	Mode 3	Mode 4	Mode 5
Open loop	1.8	1.8	1.2	1.0	1.0
Knom	47.8	47.5	33.7	3.90	11.59
Kn5.5	53.5	54.7	54.7	1.75	1.79
Kp5.5	35.5	35.9	25.3	3.64	3.63
Kp2.5	45.8	46.8	76.6	2.77	2.77
Kp10	36.4	36.8	84.3	0.40	1.00

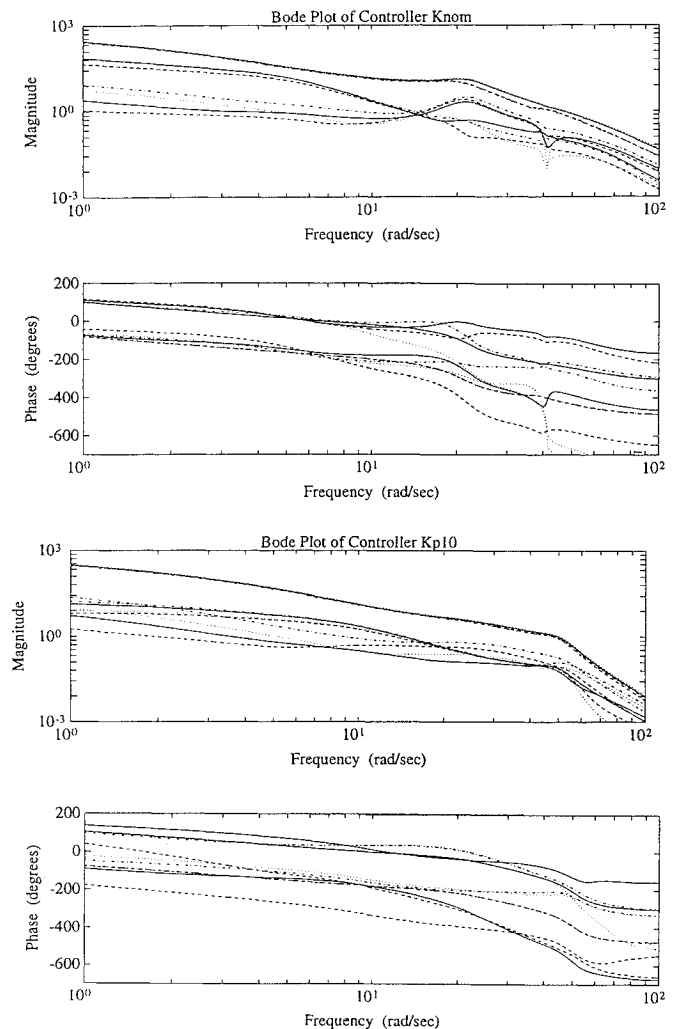


Fig. 5 Bode plots of controllers Knom and Kp10.

The Mini-Mast structure is disturbed with a 50-N, 0.1-s impulse into exciter A and the goal is to attenuate the response of the structure at bays 10 and 18. All four controllers designed for natural frequency uncertainty performed well when implemented on the system. Controller Knom is included for comparison purposes and, as one would expect, it achieved the highest level of performance (Fig. 6). Experimental data with controller Kp10 implemented on the Mini-Mast structure is shown in Fig. 7.

Comparison of the open-loop response of the structure (Fig. 6) and the closed-loop response (Figs. 7 and 8) indicate that all controllers significantly attenuate vibration. Experimental results also correlate well with time simulations of the Mini-Mast structure. Controller Kp2.5 achieves a similar level of performance as compared with controller Knom (Fig. 8). This is expected since the additional natural frequency uncertainty is relatively small, $\pm 2.5\%$. The performance level of controller Kp10, designed for $\pm 10\%$ uncertainty in the first five natural frequencies, is slightly degraded from both controllers Kp2.5 and Knom (Figs. 7 and 8). Closed-loop performance

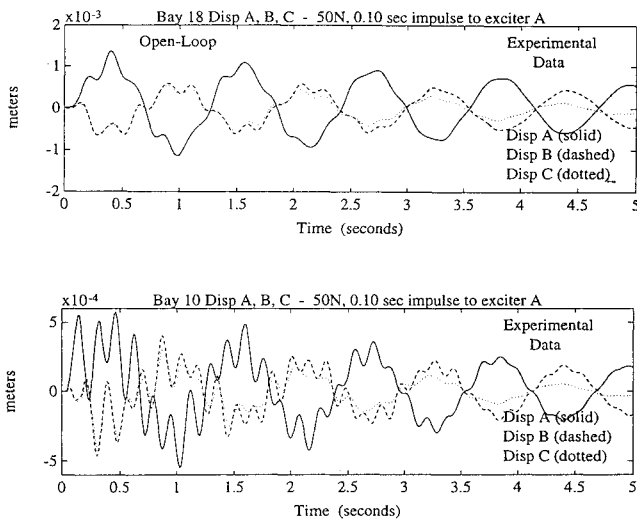


Fig. 6 Mini-Mast open-loop experimental displacement responses of bays 18 and 10.

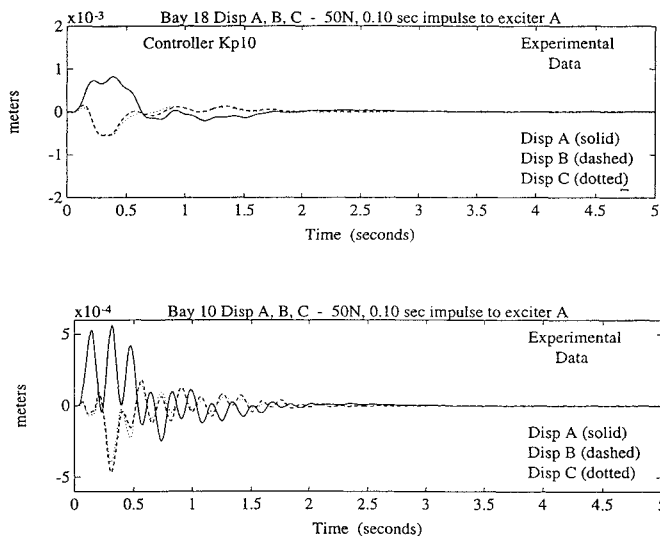


Fig. 7 Experimental displacement responses of bays 18 and 10 with Kp10 implemented.

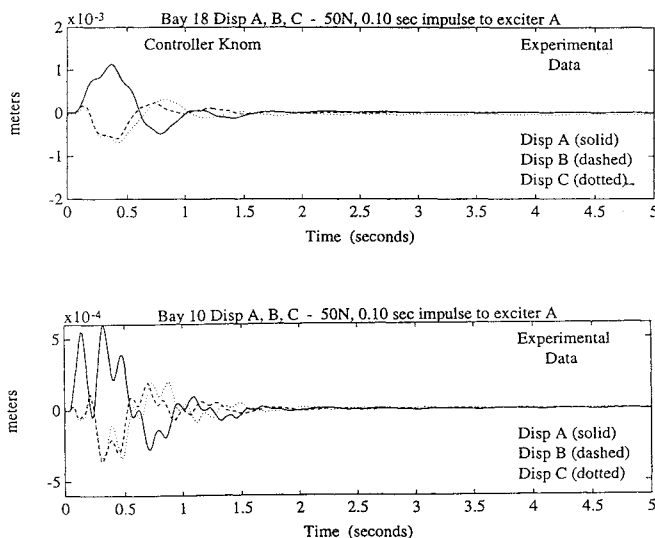


Fig. 8 Experimental displacement responses of bays 18 and 10 with Knom implemented.

is sacrificed in order to be robust to errors in natural frequencies of $\pm 10\%$. All of the controllers command less than $+50$ N/m of torque from the TWAs during the experiments.¹² Hence, we have shown that for this problem controllers can be synthesized directly for uncertainty in structural natural frequencies using the μ framework, though performance is sacrificed to achieve the additional robustness of the control designs.

VII. Summary and Conclusions

This paper employs the μ framework to synthesize controllers for a flexible structure by directly incorporating knowledge of the modeling errors in the natural frequencies in the problem formulation. The ability to accurately include these errors leads to controllers that are less sensitive and more robust to such model inaccuracies.

It is shown that complex μ -synthesis techniques can be used to intelligently account for these variations in natural frequency in the design process. A set of controllers are designed for different levels of errors in the structural natural frequencies and perform, as predicted, when implemented on the Mini-Mast experimental structure. This further validates the proposed approach.

Recently advances in the computation of the structured singular value (μ) have been made that provide tighter bounds for the analysis of systems in the presence of real and complex uncertainty. These techniques are employed to analyze the controllers synthesized to be robust to real parametric uncertainty in the control design model and validate that for this problem the above approach handles the real parameter variations with little conservatism.

It is important to note again that all controllers synthesized for the system with uncertainty in the natural frequencies used an *incorrect* model of the Mini-Mast structural natural frequencies. These experimental results are impressive, since they indicate that this methodology enabled us to design high-performance controllers despite a low-fidelity model.

Acknowledgments

The authors acknowledge the generous financial support from the National Science Foundation (ECS-9110254), NASA Langley (NAG-1-967 and NAG-1-821), and the University of Minnesota McKnight Land-Grant Professorship, and the support of the California Institute of Technology. The authors also thank Kyong Lim and Peiman Maghami for many useful discussions and Keith Belvin, Sharon Tanner, Jeff Sulla, and Rudeen Smith-Taylor for their assistance in carrying out the experiments.

References

- ¹Balas, M. J., "Modal Control of Certain Flexible Dynamic Systems," *SIAM Journal on Control and Optimization*, Vol. 16, No. 3, 1978, pp. 450-462.
- ²Joshi, S., and Groom, N. J., "Stability Bounds for the Control of Large Space Structures," *Journal of Guidance, Control, and Dynamics*, Vol. 2, No. 4, 1979, pp. 349-351.
- ³Balas, G. J., and Doyle, J. C., "Robust Control of Flexible Modes in the Controller Crossover Region," *Journal of Guidance, Control, and Dynamics*, Vol. 17, No. 2, 1994, pp. 370-377.
- ⁴Collins, E. G., Jr., King, J. A., Phillips, D. J., and Hyland, D. C., "High Performance, Accelerometer-Based Control of the Mini-Mast Structure," *Journal of Guidance, Control, and Dynamics*, Vol. 15, No. 4, 1992, pp. 885-892.
- ⁵How, J. P., and Hall, S. R., "Application of Popov Controller Synthesis to Benchmark Problems with Real Parameter Uncertainty," *Journal of Guidance, Control, and Dynamics*, Vol. 17, No. 4, 1994, pp. 759-768.
- ⁶Young, P. M., "Robustness with Parametric and Dynamic Uncertainty," Ph.D. Dissertation, California Inst. of Technology, Pasadena, CA, May 1993.
- ⁷Safanov, M. G., and Chiang, R. Y., "Real/Complex K_m -Synthesis Without Curve Fitting," *Control and Dynamical Systems*, Vol. 56, Academic, New York, pp. 303-324, 1993.
- ⁸Smith, R. S., Chu, C. C., and Fanson, J. L., "The Design of H_∞ Controllers for an Experimental Non-collocated Flexible Structure Problem," *IEEE Transactions on Control System Technology*, Vol. 2, No. 2, pp. 101-109, 1993.
- ⁹Balas, G. J., "Control Design for Flexible Structures: Theory and Experiments," Ph.D. Dissertation, California Inst. of Technology, Pasadena, CA, Jan. 1990.
- ¹⁰Pappa, R., Sulla, J., et al., "Minimast CSI Testbed: User's Guide," NASA Langley Research Center, Hampton, VA, March 1989.

¹¹Hsieh, C., Kim, J. H., and Skelton, R. E., "Closed-Loop Lab Tests of NASA's Mini-Mast," *Proceedings of the American Control Conference*, Vol. 2, 1990, pp. 1435-1440.

¹²Balas, G. J., Young, P., and Doyle, J. C., " μ Based Control Design as Applied to Large Space Structures: Control Design for the Minimast Facility," NASA CSI/GI Final Rept., NAG-1-967, 1992.

¹³Fan, M. K. H., Tits, A. L., and Doyle, J. C., "Robustness in the Presence of Mixed Parametric Uncertainty and Unmodeled Dynamics," *IEEE Transactions on Automatic Control*, Vol. AC-36, 1991, pp. 25-38.

¹⁴Young, P. M., and Doyle, J. C., "Computation of μ with Real and Complex Uncertainties," *Proceedings of the IEEE Conference on Decision and Control*, Vol. 3, 1990, pp. 1230-1235.

¹⁵Balas, G. J., Doyle, J. C., Glover, K., Packard, A. K., and Smith, R., *μ -Analysis and Synthesis Toolbox: User's Guide*, MUSYN and The Mathworks, Natick, MA, Dec. 1990.

¹⁶Doyle, J. C., "Analysis of Feedback Systems with Structured Uncertainty," *IEEE Proceedings*, Part D, Vol. 129-6, 1982, pp. 242-250.

¹⁷Packard, A. K., and Doyle, J., "The Complex Structured Singular Value," *Automatica*, Vol. 29, No. 1, 1993, pp. 71-109.

¹⁸Young, P. M., Newlin, M. P., and Doyle, J. C., " μ Analysis with Real Parametric Uncertainty," *Proceedings of the IEEE Conference on Decision*

and Control, Vol. 3, 1991, pp. 1251-1256.

¹⁹Doyle, J. C., Glover, K., Khargonekar, P. P., and Francis, B. A., "State-Space Solutions to Standard H_2 and H_∞ Control Problems," *IEEE Transactions on Automatic Control*, Vol. AC-34, No. 8, 1989, pp. 831-847.

²⁰Doyle, J. C., Lenz, K., and Packard, A. K., "Design Examples Using μ Synthesis: Space Shuttle Lateral Axis FCS During Reentry," *Proceedings of the IEEE Conference on Decision and Control*, Vol. 4, Dec. 1986, pp. 2218-2223.

²¹Sparks, A., and Banda, S. S., "Application of Structured Singular Value Synthesis to a Fighter Aircraft," *Journal of Guidance, Control, and Dynamics*, Vol. 16, No. 5, 1993, pp. 940-947.

²²Stein, G., and Doyle, J. C., "Beyond Singular Values and Loop Shapes," *Journal of Guidance, Control, and Dynamics*, Vol. 14, No. 1, 1991, pp. 5-16.

²³Packard, A. K., Doyle, J. C., and Balas, G. J., "Linear, Multivariable Robust Control with a μ Perspective," *ASME Journal of Dynamics, Measurements and Control, Special Edition on Control*, Vol. 115, No. 2b, 1993, pp. 426-438.

²⁴Morton, B., and McAfoos, B., "A Mu-Test for Robustness Analysis of a Real Parameter Variation Problem," *Proceedings of the American Control Conference*, Boston, Vol. 1, 1985, pp. 135-138.